



University
of Glasgow

Martinez, A., Aldegunde, M., Brown, A. , Roy, S. , and Asenov, A.
(2012) *NEGF simulations of a junctionless Si gate-all-around nanowire transistor with discrete dopants*. Solid-State Electronics, 71 . pp. 101-105. ISSN 0038-1101

<http://eprints.gla.ac.uk/63791/>

Deposited on: 16th May 2012

NEGF simulations of a junctionless Si gate-all-around nanowire transistor with discrete dopants

A. Martinez¹, A. R. Brown¹, S. Roy¹ and A. Asenov^{1,2}

¹ Device Modelling Group, School of Engineering, University of Glasgow, G12 8LT, UK

² Gold Standard Simulations, Ltd., Rankine Building, Oakfield Avenue, Glasgow, G12 8LT, UK

1. Abstract

We have carried out 3D Non-Equilibrium Green Function simulations of a junctionless gate-all-around n-type silicon nanowire transistor of $4.2 \times 4.2 \text{ nm}^2$ cross-section. We model the dopants in a fully atomistic way. The dopant distributions are randomly generated following an average doping concentration of 10^{20} cm^{-3} . Elastic and inelastic Phonon scattering is considered in our simulation. Considering the dopants in a discrete way is the first step in the simulation of random dopant variability in junctionless transistors in a fully quantum mechanical way. Our results show that, for devices with an “unlucky” dopant configuration, with a starvation of donors under the gate, the threshold voltage can increase by a few hundred mV relative to devices with a more homogeneous distribution of dopants.

2. Introduction

Junctionless Field Effect Transistors (JLFET) [1-2] have been proposed as an alternative to the standard minority-carrier channel MOSFETs at the end of the road map. As transistor dimensions scale down to tens of nanometres it became increasingly complicated to control the dopants at the source/channel and channel/drain boundaries. Another related problem is the intrinsic discreteness of dopants, which makes these boundaries less well defined at the nanoscale. As the JLFET is doped all the way through from source/channel/drain at the same doping concentration it is argued that it will not suffer of variability coming from fluctuations in the effective channel length, which becomes important at channel lengths of approximately 20 nm for conventional silicon transistors. Recently, a paper from the Tyndall Institute [3] has shown, experimentally and theoretically, the potential of the JLFET. A substantial amount of theoretical work has been done in studying the performance of trigate FETs and nanowires. This work ranges from semi-classical transport studies [4] to full-band quantum transport analysis [5].

Substantial work on the impact of random discrete dopants on the performance of MOSFET transistors has been carried out [6-10]. This work has made use of

Drift-diffusion, Monte Carlo and the Non-Equilibrium Green function (NEGF) carrier transport models.

Gate-all-around (GAA) nanowire transistors have a superior electrostatic integrity compared with the standard planar MOSFET architecture. When the nanowire cross-section becomes smaller than 10 nm, quantum confinement becomes important and a proper description of the sub-bands is necessary in order to properly describe quantum capacitances and the quasi-1D density of states. Furthermore, at channel lengths of less than 20 nm the tunnelling component of the source-drain current cannot be neglected [11]. Semi-classical simulation based on a Boltzmann description of the transport cannot capture the source-drain tunnelling.

In this work we use the NEGF formalism to carry out simulations of the transfer characteristics of a junctionless Si GAA nanowire transistor. We consider the impact of the random discrete dopants in the active region of the device. The random dopants are introduced by using the methodology reported in [8]. Phonon scattering is included through self-energies in the self-consistent Born approximation. We use bulk phonons, but deformation potential parameters are taken from [12]. These parameters reproduce the phonon-limited mobility for a broad range of nanowire cross-sections [13].

3. Device and Transport model

A junctionless Si GAA nanowire transistor with n-type doping concentration of 10^{20} cm^{-3} , $4.2 \times 4.2 \text{ nm}^2$ cross-section and 20 nm channel length has been used in this work. The total length of the simulated device is 60 nm. The device doping is considered discrete except in a 10 nm region close to the S/D contacts. Acoustic and optical phonon scattering are considered in the whole device. The self-consistent Born approximation is used to calculate the electron-phonon (e-p) self-energies. Inter-band, as well as intra-band, transitions have been considered in our simulations. The real part of the e-p self-energy has been neglected at this stage. An in-house NEGF simulator [14] based in an efficient coupled-mode approach using a recursive algorithm is used. This simulator has been recently benchmarked

[14] with our full 3D real-space NEGF simulator [15]. The Hamiltonian is written in the effective mass approximation. We consider here the three X valleys due to the relatively large cross-section of the nanowire. The nanowire axis is oriented in the $\langle 100 \rangle$ direction. The effective electron masses are the same as the bulk masses.

4. Simulations and Results

Five devices with randomly generated dopants that introduce differences in the realisation of disorder have been simulated. All the simulations are carried out at 50 mV drain bias as we want to demonstrate the possibility to simulate such a small device with a pure atomistic doping. The transfer characteristics are shown in Fig. 1. There are substantial fluctuations in the threshold voltage, and also variation in sub-threshold slope and drain current. The important message is that due to the small size of the cross-section and the relatively good electrostatic control, the absence of a few donors at the middle of the channel will cause doping starvation in the channel.

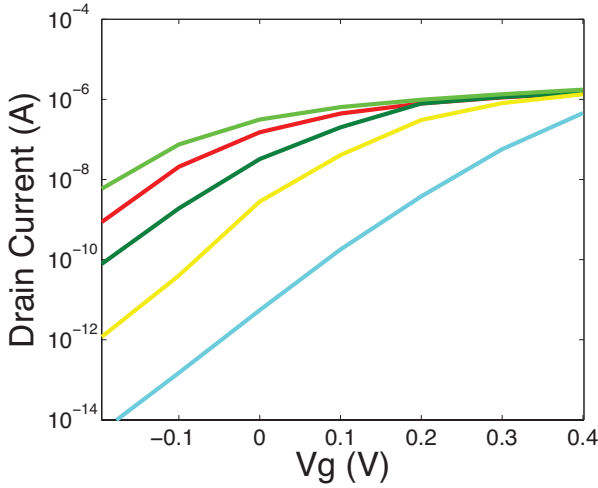


Fig. 1: Current voltage characteristics for five devices which differ in the discrete dopant distributions. The distributions are randomly generated based on a uniform donor doping of 10^{20} cm^{-3} . The drain voltage is $V_D = 50 \text{ mV}$.

Fig. 2 shows the electron density at high gate ($V_g = 0.4 \text{ V}$) for a device with lower (upper panel) and higher (lower panel) threshold voltage respectively. It is visible in the lower panel that the electron density is cut from the middle of the channel for this device as a consequence of the lack of dopants in that region. Therefore, the drain current is very low in this device. This effect produces threshold voltage shifts of hundreds of mV. Threshold voltage fluctuations as large as one volt have been experimentally observed in SOI MOSFETs due to random discrete dopants [16]. As we have not performed a full statistical study the high threshold voltage device may be an “unlucky device”

which starves from the lack of donors in the channel. However, from the point of view of solely the number of dopants this is not an extreme device, having less than a 2σ deviation from the expected number of dopants in the channel. It is the lack of dopants in the critical region under the gate that is responsible for the dramatic increase in V_T .

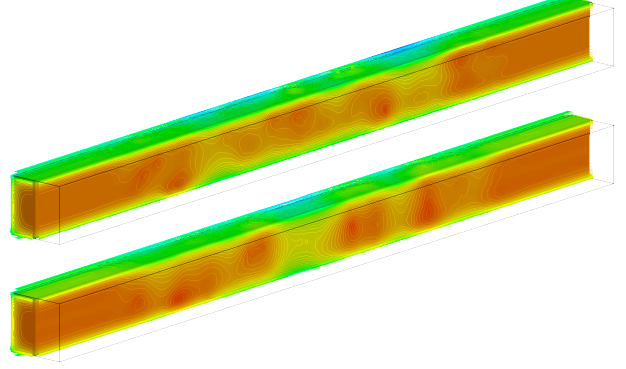


Fig. 2: The electron density along the transistor at $V_g = 0.4 \text{ V}$. Upper panel for a device with 68 dopants in the discrete doping region and low threshold voltage. Lower panel for a device with 55 dopants and high threshold voltage. Note the low electron density in the mid-channel for the lower panel device.

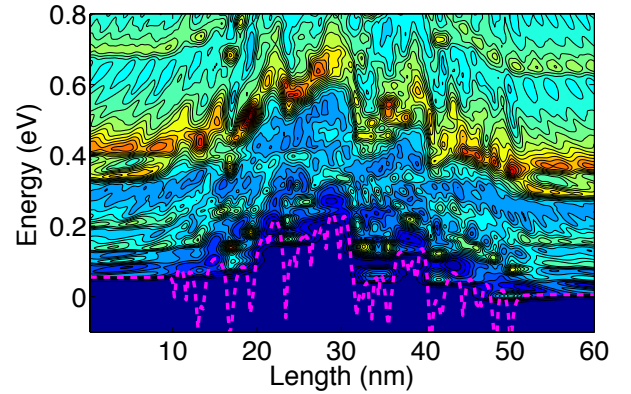


Fig. 3: Local density of states at $V_g = 0.0 \text{ V}$ for the device corresponding to the upper panel of Fig. 2. The first sub-band is shown as a reference.

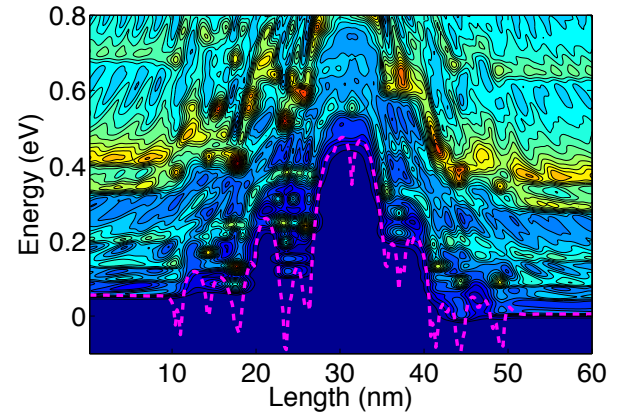


Fig. 4: Local density of states at $V_g = 0.0 \text{ V}$ for the device of the lower panel of Fig. 2. The first sub-band is shown as a reference.

Figs. 3 and 4 show the local density of states at zero gate bias ($V_g=0.0V$) for the high and low current device presented in Fig. 2. The lowest sub-band is shown in order to illustrate the effective source/drain barrier, which the electron sees in the longitudinal direction. As can be seen by comparing Fig. 3 (high current) with Fig. 4 (low current) there is a difference of a few hundred meV between the corresponding tops of the barrier. This explains the lower threshold voltage in the device of Fig. 3 compared to the device in Fig. 4. The presence in the LDOS of quasi-bound states / resonances are a signature of the localized dopant potential and have been extensively investigated [17]. The presence of more Coulomb wells in Fig. 3 than Fig. 4 at the middle of the channel confirms our finding of the lack of dopants in the middle region. An isolated dopant at the middle of the channel close to one of the Si/SiO₂ interfaces can have a lesser effect on the potential barrier as is demonstrated in Fig. 4.

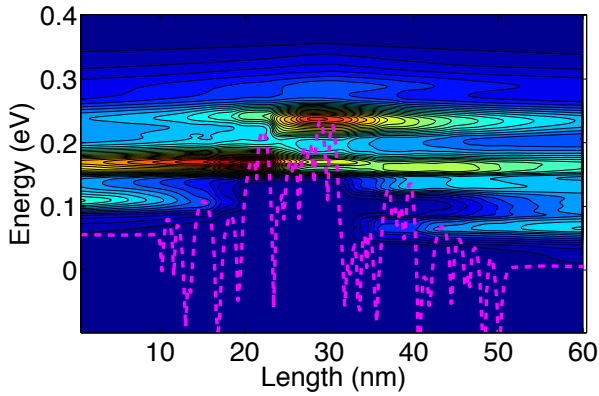


Fig. 5: Current spectrum for the low threshold voltage device of Fig. 3, at $V_g=0.0$ V. The transition of electrons by interaction with optical phonons of energy 62 meV are clearly seen in the figure. The source electrons are heated and the electrons reaching the drain are cooling down.

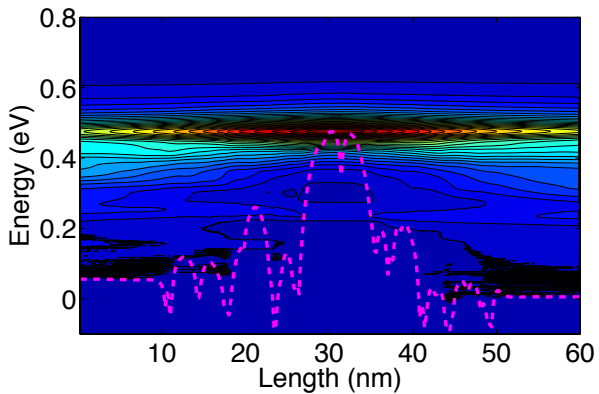


Fig. 6: Current spectrum for the high threshold voltage device of Fig. 4, at $V_g=0.0$ V. The heating of electrons at the source and cooling at the drain is reduced compared to the case of Fig. 5.

Figs. 5 and 6 show the corresponding current spectra for the devices of Figs. 3 and 4 respectively. The use of inelastic phonon scattering in the NEGF simulation allows the electrons in the channel to change their energy, unlike in ballistic simulations. Our simulations then allow for the phonon-induced broadening of the electron states and for the introduction of de-coherence. Because the total length of the wire is 60 nm there is a substantial reduction in the current due to the phonon scattering as has been demonstrated elsewhere [12, 18]. In Fig. 5 the spectrum of the current splits in two as a consequence of the 62 meV optical phonon. This mechanism allows electrons with energy substantially lower than the barrier to participate in the current and also allows for the relaxation of the hot electrons arriving at the drain. Fig. 5 also indicates that tunnelling is mediated by inelastic phonon scattering. Resonant states allow the electrons to spend more time at a particular location, and consequently increase the probability of phonon absorption / emission in that particular region of the device. This is clearly visible in Fig. 3 between 20 and 30 nm.

5. Conclusions

3D quantum transport simulations of a junctionless GAA nanowire transistor have been carried out using the Non-Equilibrium Green Function formalism. We have used an efficient coupled-mode-space implementation which is less computationally expensive than a full 3D real-space approach. The dopants in the active region of the transistor are treated discretely and the number and configuration are generated randomly and follow a Poisson distribution corresponding to the 10^{20} cm⁻³ average doping concentration. Electron phonon scattering is introduced through self-energies in the self-consistent Born approximation. The real part of the self-energy is not considered, as that would increase computational time excessively. The imaginary part is the one responsible for de-coherence and is the one that is usually considered in Monte Carlo transport simulations to treat electron-phonon scattering.

We found large fluctuations in the threshold voltage, mainly due to the potential lack of donors in the middle of the device (under the central gate region). The simulations show variations as large as 300 mV. This starvation of donors in the gate region could be less severe with increasing cross-section.

Finally, we found that the efficiency with which phonons can heat or cool the electrons, and therefore the relaxation mechanisms, are very dependent on the particular scattering mechanism and electron density of states. Quasi-bound states and resonances generated by the local potential of the impurities can enhance local absorption or emission processes, producing regions of local cooling or heating, as have been demonstrated in resonant tunnelling diodes [19].

References

- [1] J. E. Lilienfeld, Method and apparatus for controlling electric current. US patent 1,745,175 (1925).
- [2] J. E. Lilienfeld, Device for controlling electric current. US patent 1,900,018 (1928)
- [3] J. -P. Colinge, C. -W. Lee, A. Afzalian, N. D. Akhavan, R. Yan, I. Ferain, P. Razavi, B. O'Neill, A. Blake, M. White, A. -M. Keleher, B. McCarthy, and R. Murphy, *Nat. Nanotechnol.* 5, 225 (2010).
- [4] C. W. Lee, *et al.* Junctionless multigate field-effect transistor, *Appl. Phys. Lett.* 94, 053511 (2009).
- [5] L. Ansari et al Simulation of Junctionless Si nanowire transistors with 3nm gate length, *App. Phys Lett.*, 97, 062105 (2010)
- [6] A. Asenov, G. Slavcheva, A.R. Brown, J.H. Davies and S. Saini, Increase in the random dopant induced threshold fluctuations and lowering in sub-100 nm MOSFETs due to quantum effects: a 3-D density-gradient simulation study, *IEEE Trans Electron Devices* 48 (4) (2001), pp. 722–729
- [7] A. Asenov, Random dopant induced threshold voltage lowering and fluctuations in sub 0.1 μm MOSFETs: A 3-D 'atomistic' simulation study, *IEEE Trans Electron Devices* 45 (12), pp. 2505–2513, (1998)
- [8] N. Seoane, A. Martinez, A. R. Brown, J. R. Barker and A. Asenov, "Current Variability in Si Nanowire MOSFETs due to Random Dopants in the Source/Drain Regions: A Fully-3D NEGF Simulation Study", *IEEE Trans. Electron Devices*, vol. 56, no. 7, pp. 1388-1395, 2009.
- [9] Asenov, A. R. Brown, G. Roy, B. Cheng, C. Alexander, C. Riddet, U. Kovac, A. Martinez, N. Seoane and S. Roy, Simulation of Statistical Variability in Nano-CMOS Transistors using Drift-Diffusion, Monte Carlo and Non-Equilibrium Green's Function techniques, Accepted in *Journal of Computational Electronics* (2009).
- [10] R. Yang et. al. Sensitivity of trigate MOSFETs to random dopant induced threshold voltage fluctuations, *Solid-State Electronics*, 52, p. 1872-1876, (2008).
- [11] A. Martinez, N. Seoane, A. R. Brown and A. Asenov, "A detailed 3D-NEGF simulation study of tunnelling in *n*-Si nanowire MOSFETs", proceedings IEEE Silicon Nanoelectronics Workshop, Honolulu, USA, June 2010
- [12] S. Jin, Y. J. Park, and H. S. Min, "A three-dimensional simulation of quantum transport in silicon nanowire transistor in the presence of electron-phonon interactions," *Journal of Applied Physics*, vol. 99, no. 12, p. 123719, 2006.
- [13] M. Aldegunde, A. Martinez and A. Asenov, "Impact of scattering on the performance of a Si GAA Nanowire FET: from diffusive to ballistic regime", Proceedings of IWCE, 14th International Workshop on Computational Electronics, Pisa, Italy 2010.
- [14] A. Martinez, N. Seoane, A. R. Brown, and A. Asenov, A comparison between a fully-3D real-space versus coupled mode-space NEGF in the study of variability in gate-all-around Si nanowire *MOSFET*, *SISPAD IEEE*, Abstract Proceeding (2009).
- [15] A. Martinez, M. Bescond, J. R. Barker, A. Svizhenko, M. P. Anantram, C. Millar and A. Asenov, "A self-consistent 3D-Full Real Space NEGF Simulator for studying Nonperturbative effect in Nano-MOSFETs", *IEEE Trans. Electron Devices*, vol. 54, no. 9, pp. 2213-2222, 2007.
- [16] R. Wacquez *et al* "Single dopant impact on electrical characteristics of SOI NMOSFETs with effective length down to 10nm, pages 193-194 proceedings of the 2010 Symposium on VLSI Technology, Honolulu, USA.
- [17] A Martinez, J R Barker, N Seoane, A R Brown and A Asenov, "Dopants and roughness induced resonances in thin Si nanowire transistors: A self-consistent NEGF-Poisson study", *J. Phys.: Conf. Ser.* 220 012009 (2010).
- [18] M. Luisier and G. Klimeck, "Atomistic full-band simulations of silicon nanowire transistors: Effects of electron-phonon scattering", *Phys. Rev. B*, vol. 80, no. 15, Oct. (2009).
- [19] R. Lake, S. Datta, Energy balance and heat exchange in mesoscopic system, *Phys. Rev. B.* 46, 4567, 1992.